

Communication

# An Efficient Catalyst Prepared from Residual Kaolin for the Esterification of Distillate from the Deodorization of Palm Oil

Alex de Nazaré de Oliveira <sup>1,2,3,\*</sup>, Irlon Maciel Ferreira <sup>3</sup> , David Esteban Quintero Jimenez <sup>3</sup>,  
Fernando Batista Neves <sup>3</sup>, Linéia Soares da Silva <sup>4</sup>, Ana Alice Farias da Costa <sup>1,2</sup>, Erika Tallyta Leite Lima <sup>1,2</sup>,  
Luíza Helena de Oliveira Pires <sup>5</sup>, Carlos Emmerson Ferreira da Costa <sup>1,2</sup>, Geraldo Narciso da Rocha Filho <sup>1,2</sup>   
and Luís Adriano Santos do Nascimento <sup>1,2,\*</sup> 

- <sup>1</sup> Graduation Program in Chemistry, Federal University of Pará, Augusto Corrêa Street, Guamá, Belém 66075-110, PA, Brazil; analilice@hotmail.com (A.A.F.d.C.); erikatallyta@hotmail.com (E.T.L.L.); emmerson@ufpa.br (C.E.F.d.C.); geraldonrf@gmail.com (G.N.d.R.F.)
- <sup>2</sup> Laboratory of Oils of the Amazon, Federal University of Pará, Belém 66075-750, PA, Brazil
- <sup>3</sup> Laboratory of Biocatalysts and Applied Organic Synthesis, Chemistry Course, Federal University of Amapá, Campus University Marco Zero of Equador, Rodovia Juscelino Kubitschek de Oliveira Km 02, Zerão, Macapá 68902-280, AP, Brazil; irlon.ferreira@gmail.com (I.M.F.); derteriom@gmail.com (D.E.Q.J.); fertista3798@gmail.com (F.B.N.)
- <sup>4</sup> Federal Institute of Education, Science and Technology of Amapá, Macapá 68909-398, AP, Brazil; dasilvalineia@gmail.com
- <sup>5</sup> High School of Application, University of Pará, Belém, Pará 66095-780, CEP, Brazil; lulenapires@hotmail.com
- \* Correspondence: alexoliveiraquimica@hotmail.com (A.d.N.d.O.); adrui1@yahoo.com.br (L.A.S.d.N.); Tel.: +55-91-98171-4947 (A.d.N.d.O.)



**Citation:** de Nazaré de Oliveira, A.; Ferreira, I.M.; Jimenez, D.E.Q.; Neves, F.B.; Soares da Silva, L.; Farias da Costa, A.A.; Lima, E.T.L.; de Oliveira Pires, L.H.; Ferreira da Costa, C.E.; Narciso da Rocha Filho, G.; et al. An Efficient Catalyst Prepared from Residual Kaolin for the Esterification of Distillate from the Deodorization of Palm Oil. *Catalysts* **2021**, *11*, 604. <https://doi.org/10.3390/catal11050604>

Academic Editor: Juan Antonio Cecilia

Received: 15 April 2021  
Accepted: 3 May 2021  
Published: 7 May 2021

**Publisher's Note:** MDPI stays neutral with regard to jurisdictional claims in published maps and institutional affiliations.



**Copyright:** © 2021 by the authors. Licensee MDPI, Basel, Switzerland. This article is an open access article distributed under the terms and conditions of the Creative Commons Attribution (CC BY) license (<https://creativecommons.org/licenses/by/4.0/>).

**Abstract:** The distillate from the deodorization of palm oil (DDPO) is an agro-industrial residue, approximately 84% of which consists of free fatty acids (FFAs), which can be used for the production of fatty acid ethyl esters (FAEE). A catalyst (10HPMo/AlSiM) obtained from a waste material, Amazon *flint* kaolin, was applied in the esterification of the DDPO, reaching a conversion index of 94%, capable of maintaining satisfactory activity (>75%) after four consecutive cycles. *Flint* kaolin is therefore proven to be an efficient option in the search for new heterogeneous low-cost catalysts obtained from industrial by-products, contributing to the reduction of environmental impact and adding value to widely available wastes that would otherwise be discarded directly into the environment. Based on the catalytic results, esterification of DDPO using 10HPMo/AlSiM can be a cheaper alternative for the production of sustainable fuels.

**Keywords:** kaolin; mesoporous; heterogeneous catalyst; esterification; waste valorization

## 1. Introduction

Since the discovery of the family of mesoporous molecular sieves known as M41S in 1992 [1,2], MCM-41 (*Mobil Composition of Matter No. 41*) has been the most widely studied, due to its widerange of potential applications either as a catalyst [3] or catalytic support [4]. This is due to its combination of elevated surface areas and a well-defined pore size, which can be controlled and stabilized, while it is also easy to obtain [5,6]. The preparation of MCM-41 commonly involves sodium or ammonium hydroxide, hexadecyltrimethylammonium bromide (CTABr) as a driver and silica gel or tetraethylorthosilicate (TEOS) as a source of silica [2,6–8]. However, the use of TEOS for obtaining MCM-41 has toxic effect, and the materials involved in the process are expensive [7,9–11]. For economic and environmental reasons, efforts to find new sources of inorganic silicates containing high levels of silica at a low cost are increasing [12–14].

To circumvent such challenges, the use of alternative sources of silica, such as kaolin, to replace commercial options, applied in the synthesis of mesoporous materials, reduces the toxicity of the process and reduces costs, as they represent a natural raw material,

that is both inexpensive and widely available [4,15–18]. The preparation of mesoporous aluminosilicates from natural clay minerals has been investigated, due to the high silicon and aluminum content used in the synthesis of these mesoporous materials [15,19,20].

In the Amazon, the production of kaolin generates significant amounts of tailings, among which *flint* kaolin, FK, is deposited in the mine after the exploitation of soft kaolin, generating major environmental impacts, as it mainly comprises clay mineral kaolin, and contains high levels of silicon, aluminum, titanium and iron [21–23]. These low-quality kaolinitic tailings have been used as a raw material in various chemical processes, including as a catalyst [18,22,24–26], catalytic support [4,27], in zeolite synthesis [21,28,29] and as mesopore [15–17].

New heterogeneous catalysts and catalytic supports have been developed for application in the esterification of FFAs, including mesoporous silica [4,15–17,30], clay minerals [4,18,22,24–26,31] and several catalytic supports with heteropoly acids (HPAs) [4,15,30–35]. The HPAs are notable due to their high Brønsted acidity and redox properties [36,37], which favor the protonation of the carbonyl of FFAs during alcoholic esterification [4,15,30,31,34]. Supporting an HPA in a suitable matrix is known to control the strength and distribution of its active sites [36–38], and it can be applied in a wide range of heterogeneous reactions, including the esterification of low-cost raw materials with high FFA levels for the clean and efficient synthesis of mono alkyl esters (biodiesel), and with water as a by-product [4,30,31,33,34,39–44].

Several previous studies have investigated the possibility of using low-cost raw materials [4,16,26,31,45–48] which can potentially be applied in the synthesis of monoalkyl esters [4,30,31,33,34,39–44]. Notable among these is a by-product from the refining of vegetable oil, a distillate from the deodorization of palm oil (DDPO), around 84% of which is made up of FFAs [4,16,26,31]. The use of these FFAs to generate coproducts with a higher added value is a viable option for the mitigation of possible environmental impacts due to the disposal of such waste [49]. In this case, heterogeneous acid catalysts can esterify the FFAs into esters [4,16,26,31,50,51], and offer advantages such as separation and recovery at the end of the process, as well as subsequent reuse capacity, while avoiding the generation of secondary products and toxic effluents [4,30,31,34,40,43,52].

The use of 12-molybdophosphoric acid ( $H_3PMo_{12}O_{40}$ , HPMo) functionalized on silica (alternative source, FK) with a well-ordered hexagonal arrangement as an efficient acid catalyst for the esterification of eugenol, was recently reported by our group [15]. This study focused on the synthesis, characterization and application of a catalytic material as a contribution to Green Chemistry, since this catalyst comes from residues which are abundant in the Amazon region [15]. Therefore, the present work aimed to apply this mesoporous material, with an ordered hexagonal phase, in addition to describing a purpose for FK, to produce a low cost catalyst, anchored with HPMo in its mesopores [15], in the DDPO ethanolic esterification reaction. The raw materials used were chosen due to their low-cost and wide availability as waste in the Amazon region. Ethanol was used as it is produced from renewable sources, unlike methanol, which is generally derived from fossil sources [4,31,53]. The reaction between ethanol and DDPO (as a source of FFAs) was chosen as both reagents have greener properties and are widely available for the production of renewable FAEE.

## 2. Results and Discussion

### 2.1. Influence of Time on the Esterification Reaction of DDPO

The duration of the reaction process strongly influences the consumption of reagents and the formation of products of interest. As expected, for the esterification reaction, the initial conversion of 62% obtained 30 min after the start of the reaction gradually increased over time (Figure 1a). The reaction conversion percentage was higher in the 30 to 120 min intervals, with conversions varying from 62 to 94%, respectively. However, from 120 to 150 min, the conversion remained practically unchanged. The results obtained herein after 2 h of reaction were better than those obtained by Pires et al. [4] using 12-tungstophosphoric

acid supported on metakaolin waste (25%HPW/MK700) to catalyze DDPO, where after 2 h an 83% conversion to FAEE was obtained. Although Aranda et al. [54] achieved a 90% conversion of DDPO in 1 h of reaction using  $H_2SO_4$  as a catalyst, the disadvantages of the homogeneous sulfuric acid catalyst are well known, such as its non-reusability and corrosion of equipment characteristics. The results achieved in this study still provided a better reaction time ( $\leq 2$  h) than other previously published studies [26,34,52,53,55,56].

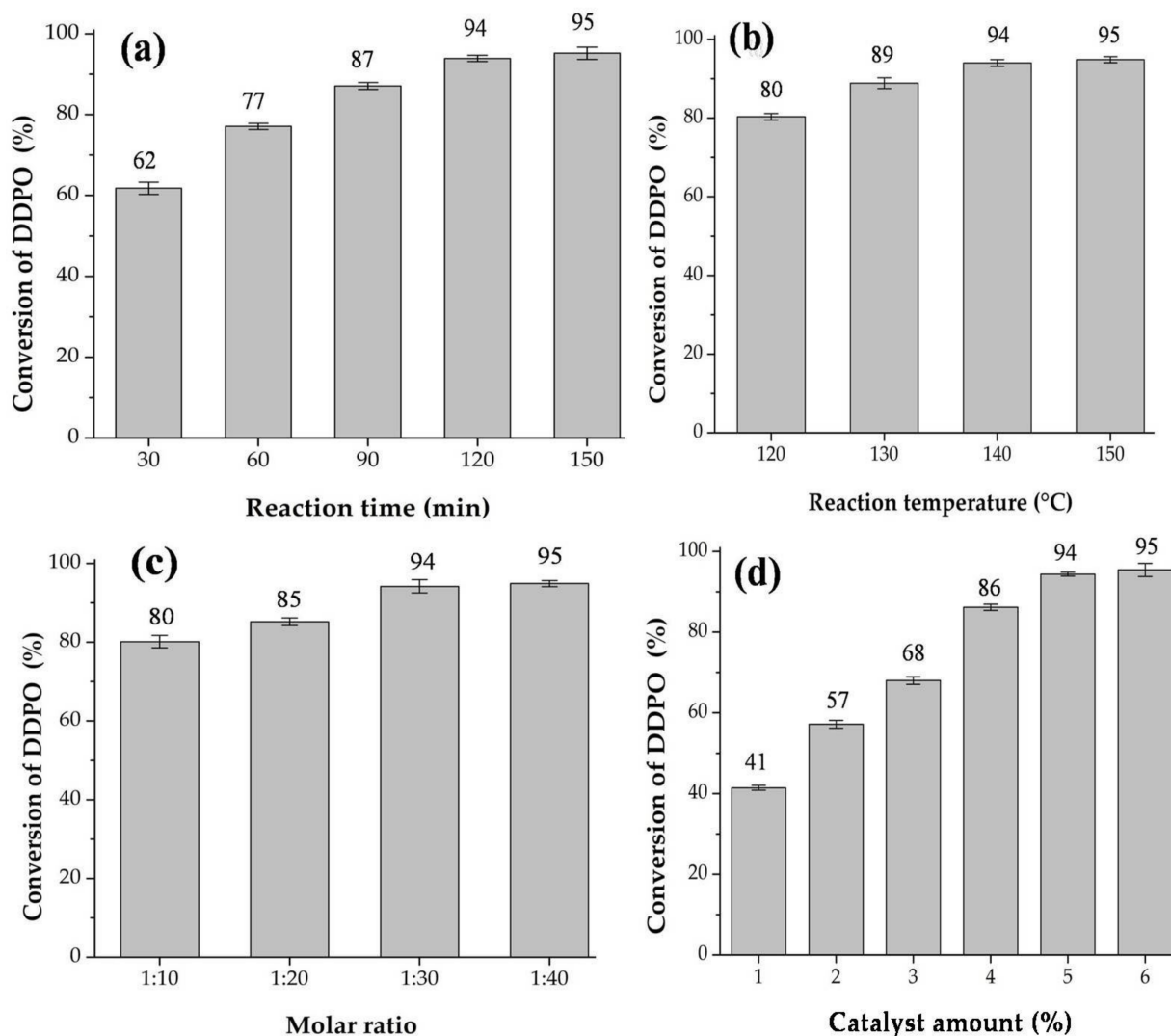


**Figure 1.** Influence of reaction parameters on esterification: (a) reaction time, (b) reaction temperature, (c) molar ratio DDPO: EtOH, (d) Catalyst amount. Reaction conditions: 1:30 molar ratio (DDPO: EtOH), reaction temperature 140 °C, reaction time 2 h and 5% catalyst.

## 2.2. Influence of Temperature on DDPO Esterification Reaction

The effect of the reaction temperature was investigated, and the results are shown in Figure 1b. The reaction was studied by varying the temperature from 120 to 150 °C without altering the other experimental conditions. An 80% increase in conversion was observed at 120 °C. At higher temperatures, the reaction attained equilibrium, with a conversion of 94% at 140 °C. These results show that higher temperatures increase the kinetic energy of the molecules, which accelerates the reaction, facilitating the mass transfer between the reactants and the catalyst surface [57]. Therefore, the ideal reaction temperature was determined to be 140 °C, lower than that required for other catalysts (150 to 210 °C) in similar reactions [4,26,31,33,34,44,52,53,56,58].

### 2.3. Influence of the Molar Ratio of DDPO and Ethanol in the Esterification Reaction

Theoretically, the esterification reaction occurs at a stoichiometric ratio of 1 mol of FFA to 1 mol of alcohol, generating 1 mol of ester and 1 mol of water. As the esterification reaction is reversible (hydrolysis), an excess of alcohol is required to drive the reaction towards ester formation and avoid hydrolysis [4,22,24,26,31,51].

To study the influence of the substrate molar ratio, the reaction was carried out by varying the DDPO: EtOH molar ratio from 1:10 to 1:40. According to Figure 1c, the conversion of DDPO increased with the molar ratio, reaching a maximum value of 94% with the DDPO: EtOH molar ratio of 1:30. As the molar ratio increased, however, an appreciable increase in conversion was not observed, which can be attributed to the occurrence of the reverse hydrolysis reaction of part of the esters produced in the presence of excess ethanol [4,30,31]. Thus, the 1:30 molar ratio was determined to be ideal for the esterification reaction, achieving maximum DDPO conversion. It should be stated that lower proportions, such as 1:10 and 1:20, were also used, attaining 80 and 85% conversion, respectively, showing that the 10HPMo/AlSiM catalyst maintained a strong catalytic performance. This can reduce the production costs of the process on a nonlaboratory scale, as less ethanol would be needed to promote the reaction. Even so, studies have shown that a high molar ratio of 1:30, 1:40 or 1:90 is necessary to shift the reaction balance to a direct basis, in order to achieve maximum conversion [27,31,33,34,37,38,40].

### 2.4. Influence of Amount of Catalyst on DDPO Esterification

Control experiments with AlSiM and HPMo were also carried out under optimized conditions. At first, the esterification reaction of DDPO with EtOH without a catalyst exhibited a conversion close to 20%, while the esterification reaction in the presence of AlSiM did not reach 23%. Therefore, AlSiM alone is unable to promote a high conversion during the esterification of DDPO, indicating that the catalytic activity is mainly due to the HPMo present in AlSiM, which makes 10HPMo/AlSiM highly active. The same reaction was carried out with the active amount of HPMo (64 mg) which converted 90% of DDPO in homogeneous esterification.

Figure 1d shows the variation in the conversion of DDPO based on the amount of catalyst during ethanolic esterification. The effect of the amount of the 10HPMo/AlSiM catalyst was investigated by the variation in the dosage, which varied from 1 to 6% by mass, based on DDPO mass. It was observed that the DDPO conversion increased from 41 to 94% as the catalyst dosage increased from 1 to 5%. A 4% load can be used without drastically reducing the conversion of DDPO (86%), which shows the efficiency of the catalyst. An additional increase in the amount of catalyst resulted in not significant changes in the conversion of DDPO, indicating that 5% is the catalyst dosage that ensures the appropriate number of active acid sites for the esterification of DDPO.

### 2.5. Comparison with Data from Literature

A comparison with other types of heterogeneous and homogeneous catalysts used in the esterification of FFAs described in literature was performed (Table 1). The results obtained in this study indicate that the catalyst has a strong potential for use in the esterification reaction of DDPO, a low-quality organic matter (see Table 1). The 94% observed value for the conversion to esters during the esterification of DDPO with EtOH using the 10HPMo/AlSiM catalyst is close to the values of 62% [59], 90% [54] and 99.9% [45] achieved by sulfuric acid as a catalyst, a substance which has well-known disadvantages. Similar results were obtained using solid acid catalysts such as CsHPW/MCM (92%) [60], MF9S4 (<93%) [26], BLMW (<94%) [31], with even better results than those reported for MP-S-16 (15) (<82%) [30], 25% HPW/MK700 (83%) [4] and CrWO<sub>2</sub> and CrWTiO<sub>2</sub> (<86%) [52,56]. However, the use of chromium is not environmentally friendly in comparison with the aforementioned HPMo material. H<sub>3</sub>PMo/Al<sub>2</sub>O<sub>3</sub> (97%) [33], AM41-2H-O (98%) [16], HPMo/Nb<sub>2</sub>O<sub>5</sub> (99.9%) [34] were better than the results achieved in the present study. Although all of the catalysts mentioned are reasonably efficient in the esterification

reactions of FFA residues, with high conversion to esters, in most cases, higher temperatures ( $\geq 140$  °C) and longer reaction times ( $\geq 2$  h) than those of the present study were necessary. In addition, the cost of the preparation of our material modified with HPMo was low, since it used kaolinitic residue as a precursor to aluminosilicate, and we still believe that it is more environmentally friendly.

**Table 1.** Comparison of the catalytic activity of 10HPMo/AlSiM with other catalysts for the esterification of different free fatty acids.

Catalyst	FFAs	Alcohol	M: R <sup>a</sup>	(°C) <sup>b</sup>	(h) <sup>c</sup>	(%) <sup>d</sup>	Ref.
Al-MCM-41Si/Al = 8	Palmitic	MeOH	1:60	130	2	79	[3]
25%HPW/MK700	DDPO	EtOH	1:10	200	2	83	[4]
AM41-2H-O	DDPO	MeOH	1:30	130	2	98	[16]
MF9S4	Oleic	MeOH	1:60	160	4	98.9	[22]
MF8S4M4W15	Oleic	MeOH	1:60	115	2/3	96.5	[25]
MF9S4	DDPO	MeOH	1:60	160	4	92.8	[26]
MP-S-16 (15)	CKO	MeOH	1:8	140	5	82	[30]
BLMW	DDPO	EtOH	1:30	160	2	93.3	[31]
H <sub>2</sub> SO <sub>4</sub>	Soapstock	MeOH	1:18	50	14	99.9	[45]
CrWO <sub>2</sub>	PFAD	MeOH	1:2	170	3	86	[52]
CrWTiO <sub>2</sub>	PFAD	MeOH	1:2	170	3	80	[56]
H <sub>2</sub> SO <sub>4</sub>	PFAD	MeOH	1:3	60	3	62	[59]
H <sub>2</sub> SO <sub>4</sub>	DDPO	MeOH	1:3	130	1	90	[54]
CsHPW/MCM	PFAD	MeOH	1:15	85	4	92	[60]
10HPMo/AlSiM	DDPO	EtOH	1:30	140	2.5	94	Present work

<sup>a</sup> Molar ratio; <sup>b</sup> Temperature; <sup>c</sup> Time; <sup>d</sup> Conversion of FFA, Methanol = MeOH.

Therefore, the reaction of esterification of DDPO with EtOH is accelerated by HPMo as an active species (Brønsted acid sites) in the structure of AlSiM, making the catalyst reasonably effective. The results obtained using 10HPMo/AlSiM as a catalyst for the esterification of DDPO with EtOH are largely satisfactory, as the results are similar or superior to those presented in literature using different reagents and catalysts (Table 1).

Finally, it must be noted that the costs of production of the catalyst from Amazonian FK are encouraging. The use of this waste as a raw material for a low-cost silica source for the production of catalytic supports proved to be quite feasible [15–17]. While in the reaction EtOH was also used as a solvent and DDPO by-product as FFAs, all are raw materials that have greener properties for sustainable FAEEs production [31]. Thus, the use of industrial by-products, such as FK and DDPO, in the synthesis of new mesoporous material and FAEEs makes production sustainable, reduces the environmental liabilities caused by its disposal and adds economic value to waste.

## 2.6. Catalyst Deactivation and Recyclability

Recovery, stability and reuse are important aspects of heterogeneous catalysts [30,34,37]. The reuse of 10HPMo/AlSiM in the esterification reaction was analyzed for four successive catalytic cycles under the optimal reaction conditions established in this study. The results in relation to the repeated use of the catalyst are shown in Table 2.

Table 2 also shows the results obtained for DDPO conversion using the recycled catalyst. A gradual reduction in DDPO conversion, from 94 to 74.6% in the fourth cycle, was observed, results which are still superior to those of the autocatalysis (20%), indicating that the material can be reused for several cycles and retain the potential to protonate FFAs. The TOF values followed the same trend. This reduction in catalytic activity can be attributed to factors such as loss of mass or even the blockage or destruction of pores by remaining impurities, even after the purification stage (filtration, washing and drying), in addition to the leaching of the active species of the support shown in Table 2 (as no amounts of HPMo were added to the catalyst) [15,30,31,34]. The leaching of the active species (Mo) from the reused catalyst was monitored by the XRF and UV–vis techniques [4,15,27,31,61].

**Table 2.** Properties of acidity, leaching of active species and catalyst conversion during recycling.

Cycles	(g) <sup>a</sup>	(mmol H <sup>+</sup> g <sup>-1</sup> ) <sup>b</sup>	%MoO <sub>3</sub> <sup>c</sup>	(mg) <sup>d</sup>	(μg) <sup>e</sup>	(%) <sup>f</sup>	(%) <sup>g</sup>	(min <sup>-1</sup> ) <sup>h</sup>
10HPMo/AlSiM	-	5.84	7.40	20.8	0.60	2.88	94	244
10HPMo/AlSiM R1	2.34	5.41	7.37	20.2	0.55	2.72	90	221
10HPMo/AlSiM R2	2.17	5.21	7.36	19.7	0.58	2.95	84	217
10HPMo/AlSiM R3	1.93	5.05	7.36	19.1	0.58	3.01	79	216
10HPMo/AlSiM R4	1.88	4.58	6.93	18.5	0.70	3.08	75	216

<sup>a</sup> Dry mass of the catalyst recovered after each reuse cycle for 2 h at 140 °C (the reagents were always recalculated to maintain the same conditions: DDPO: EtOH = 1: 30 and 5% catalyst); <sup>b</sup> surface acidity calculated by titration; <sup>c</sup> XRF of the catalysts after tests; <sup>d</sup> mass of HPMo anchored in AlSiM measured by UV–vis; <sup>e</sup> mass of leached HPMo detected by UV–vis; <sup>f</sup> percentage of leaching in the reaction medium; <sup>g</sup> conversion of DDPO; <sup>h</sup> TOF (turnover frequency) = ((Conversion% × moles of DDPO fed) / (No. of mol of Mo species) × (reaction time)); No. of moles of Mo species = (mass of HPMo / 1825.25) × (95.95 / 1825.25) [15,30,31], according to the results of the UV–vis analysis; R: refers to the reused catalyst.

The results of XRF analysis of the reused catalysts showed that the percentage content of MoO<sub>3</sub> in the new and reused catalysts was practically the same, until the third reuse cycle (see Supplementary Materials). Analysis of the reaction mixtures by UV–vis confirmed there was leaching of active species (Mo) of close to 3% in all the reuse cycles. This can be attributed to the loss of active sites during friction in the reactor during the reaction, and also during the recovery process [15,30,31,34]. These observations ensure that HPMo leaching from AlSiM support is within acceptable limits (3%) [15,27,31]. The acidity values of the reused catalyst measured by titration revealed a decline after each run, in comparison with the new catalyst, which was consistent with the declining values of the DDPO conversion (Table 2).

To verify the integrity of the catalyst after successive esterification reactions, it was analyzed by the XRD, DRS and FTIR techniques after a fourth reuse cycle (Figure 2a–c). Figure 2a shows the XRD of the 10HPMo/AlSiM and 10HPMo/AlSiM R4 catalysts. There was a clear reduction in peak intensity corresponding to reflection (100), followed by the absence of reflection (110, 200 and 210), a strong indication that the hexagonal mesostructure had become disordered, [4,15,62], but was still preserved [4,62]. This was expected, since the reactions were conducted under aggressive mechanical agitation and temperature conditions [15,30,37,62].

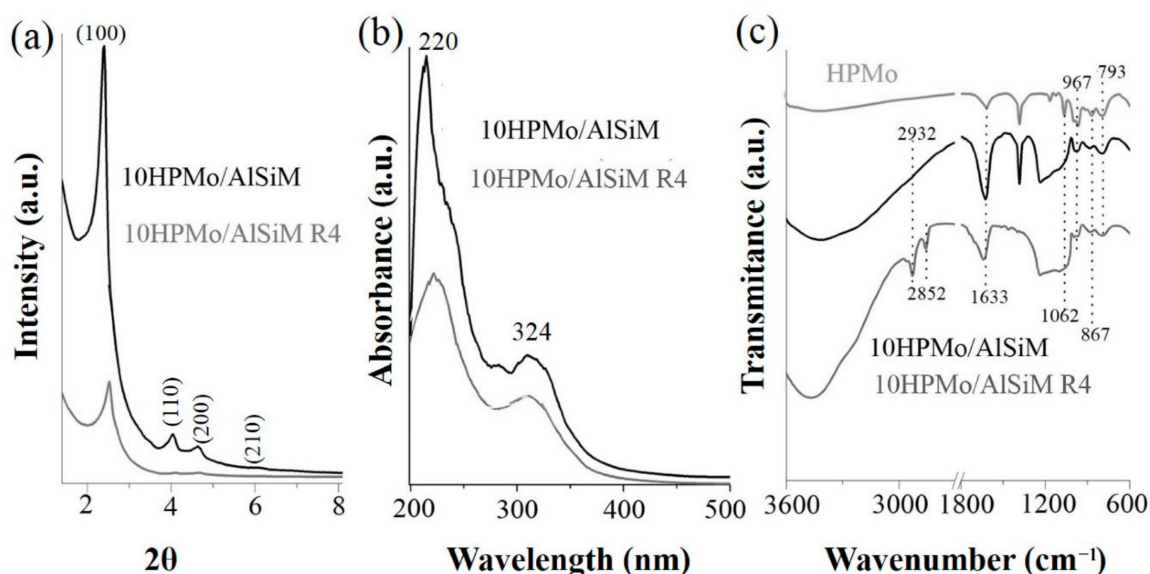


**Figure 2.** (a) Comparison of XRD standards, (b) DRS spectra, (c) FTIR spectra of the new catalyst and after the fourth reuse cycle. R: refers to the reused catalyst.

In the DRS absorption spectrum of 10HPMo/AlSiM-R4 shown in Figure 2b, broad and less intense bands appeared at 220 and 324 nm, indicating the presence of HPMo and the stability of the catalyst after the four reaction cycles [15,62–65]. Analyzing the FTIR spectra of 10HPMo/AlSiM-R4 in Figure 2c, there was a marked presence of bands in the 800 to 1100  $\text{cm}^{-1}$  range, characteristic of HPMo with a Keggin structure, which was maintained after the fourth catalytic cycle. Some new prominent adsorption bands, such as at 2932 and 2852  $\text{cm}^{-1}$ , were attributed to the symmetrical stretching of the  $\text{CH}_3$  bonds, while a very discrete band, at 1465  $\text{cm}^{-1}$ , was attributed to the asymmetric  $\text{CH}_3$  deformation. The adsorption of organic molecules in the reused catalyst can be clearly seen, and may involve impurities such as triglycerides and unsaponifiable matter present in around 16% of the DDPO [4,16,26,31]. The adsorption of these molecules on the catalyst surface contributed to the reduction of catalytic activity [31,66,67]. This is in line with studies that demonstrated that catalysts with PAHs or other anchored solid acids could be recycled and have been found to have effective recycling capacity [4,15,30,34,38].

Finally, through the use of FRX, UV-vis, DRX, DRS and FTIR techniques, it was observed that active species were still present in the material, and it was concluded that the hexagonal structure of the mesopore was preserved after the recyclability tests. From previously published works [15,19,20] and the results achieved here with 10HPMo/AlSiM, it is possible to predict the use of AlSiM, synthesized at low cost, as a catalytic support to be applied in other types of organic transformation reactions, operating in a predominantly heterogeneous phase.

### 3. Experimental Section

#### 3.1. Materials

All chemical reagents and solvents were analytical grade and used without further purification. DDPO is a residue (viscosity at 60 °C = 12.296  $\text{mm}^2 \text{s}^{-1}$ ; density at 60 °C = 0.862  $\text{g mL}^{-1}$ ; water content < 0.5%; oxidative stability > 150 h; acidity index = 177.15  $\text{mg KOH g}^{-1}$ ) consists of 84.0-wt% free fatty acid (FFA) (42% palmitic, 41% oleic, 10% linoleic, 5% stearic, 2% lauric and 1.5% myristic), 12-wt% triglycerides, diglycerides and monoglycerides and 4-wt% unsaponifiable matter [4,16,26,31], kindly donated by Companhia Refinadora da Amazônia, Agropalma S/A (Brazil). *Flint* kaolin of the Capim River Region (Pará, Brazil) was used as Si and Al source and was kindly supplied by the Institute of Geology-UFGPA, ethanol (EtOH, 98%, synthetic grade, Nuclear, São Paulo, SP–Brazil), hydrochloric acid (HCl, 37%, Fmaia, Belo Horizonte, MG–Brazil) and sodium hydroxide (NaOH, VETEC, Rio de Janeiro, RJ–Brazil). The preparation and characterization of the 10HPMo/AlSiM were described in a previous work [15].

#### 3.2. Characterization of Fresh and Reused Catalyst

The chemical compositions of the samples were obtained with Shimadzu EDX-700 energy dispersive X-ray spectrometer (EDX; EDX-700, SHIMADZU, Kyoto, Japan), with a rhodium X-ray source tube (40 kV, SHIMADZU, Kyoto, Japan). For each analysis, approximately 500 mg (powder) of each sample was deposited in a lower sample holder made of polyethylene film in order to determine the  $\text{MoO}_3$  content present in the fresh and reused catalyst.

X-ray diffraction analysis were performed on a Bruker D8 Advance diffractometer (Bruker D8Advance; Bruker Corp, Billerica, MA, USA), using powder method, at a  $1^\circ < 2\theta > 10^\circ$  interval.  $\text{Cu K}\alpha$  ( $\lambda = 1.5406 \text{ \AA}$ , 40 kV e 40 mA) radiation was used.

Diffuse ultraviolet–visible reflectance spectroscopy (DRS) readings were recorded, in the range of 200–500 nm, on a Shimadzu UV–vis model ISR-2600 Plus spectrophotometer (EDX; EDX-700, SHIMADZU, Kyoto, Japan).

Fourier transform infrared spectroscopy (FTIR) spectra were obtained from a spectrophotometer of Shimadzu (Kyoto, Japan) model IRP Prestige-21A with a resolution of 32 and 100 scans and analyzed by Thermo Electron Corporation, IR 100 model with a resolution of 4 and 32 scans. For the analysis of all materials KBr pellets were used and the spectra were obtained in the region 4000–400  $\text{cm}^{-1}$ .

The leaching of the HPMo catalysts was performed in UV–vis equipment of Thermo-scientific (Waltham, MA, USA), model Evolution array UV–vis spectrophotometer, with 200 to 600 nm scan and 30 scan resolution. The liquids were placed in a quartz tube. The quantification of the HPMo leached in the reaction medium was made using the analytical curve constructed from the postreaction solution (1 to 5  $\text{mg L}^{-1}$  of HPMo), which was diluted with 0.1  $\text{mol L}^{-1}$  HCl to avoid any hydrolysis anion  $[\text{PMo}_{12}\text{O}_{40}]^{3-}$ , with an absorbance equation ( $y = 0.0999 + 0.0025x$ ) of  $\lambda_{\text{max}} = 310$  nm and an excellent correlation coefficient ( $R^2 = 0.9999$ ) based on our previous studies [15,31].

### 3.3. Catalytic Activity

Prior to the experiments, the catalysts were activated at 130 °C for 2 h. Tests of the catalysts were conducted in one run on a PARR 4871 multi-reactor (Parr Instrument Company, Moline, IL, USA). In a typical experiment, the DDPO was mixed with alcohol at a molar ratio of 1:10, 1:20, 1:30 and 1:40 (DDPO: EtOH) and 1, 2, 3, 4, 5 and 6% *w/w* of the solid acid catalyst (as compared to the mass of DDPO). The reaction mixture was stirred (500 rpm) and heated from room temperature to 120, 130, 140 and 150 °C. Once the desired temperature was reached, the system was maintained for 30, 60, 90, 120 and 150 min, considered to be the kinetic contact time. At the end of the reaction, the catalyst was separated from the reaction medium by vacuum filtration, and the excess methanol and water produced were removed by evaporation at 120 °C. The percentage conversion of DDPO to the corresponding ester was estimated by acid measurement of the product by titration with 0.1  $\text{mol L}^{-1}$  hydroxide, according to the methods described in the literature. [4,16,26,31]. Reaction parameters such as time, molar ratio, temperature, and catalyst loading were optimized and evaluated. In addition, the recyclability of the catalyst was assessed in the DDPO esterification reaction under the same conditions listed above. At the end of each reaction cycle, the catalyst was filtered under vacuum, washed with 50 mL of ethanol to remove residues and dried at 150 °C for 12 h. The catalyst was reused in four reaction cycles.

## 4. Conclusions

Experimental investigations revealed that the 10HPMo/AlSiM catalyst exhibited excellent catalytic activity during the esterification reaction of DDPO with ethanol, reaching a conversion of 94%. The XRF, XRD, DRS and FTIR characterization results for this material confirmed the preservation of HPMo after the fourth cycle of reuse in the reaction, where it exhibited a conversion rate of over 75%. The use of two industrial by-products—*Flint* kaolin for the synthesis of mesoporous material and DDPO for the production of ethyl esters—enables sustainable production, reducing possible environmental impacts arising from their provision, in addition to adding economic value to such residues. The results obtained were comparable with previously published results on the use of this reaction and the availability of FK makes this material a promising alternative to those already used. Thus, the results obtained in the present study encourage the search for varied applications for both the 10HPMo/AlSiM catalyst and AlSiM support in oxidation reactions and heavy metal removal, among others.

**Supplementary Materials:** The following are available online at <https://www.mdpi.com/article/10.3390/catal11050604/s1>, Elemental analysis by XRF of Table 2.

**Author Contributions:** Conceptualization, L.A.S.d.N.; methodology, C.E.F.d.C. and G.N.d.R.F.; formal analysis, A.d.N.d.O., L.H.d.O.P., F.B.N., D.E.Q.J., L.S.d.S., A.A.F.d.C., and E.T.L.L.; investigation, A.d.N.d.O., E.T.L.L. and L.H.d.O.P.; resources, I.M.F., D.E.Q.J. and C.E.F.d.C.; data curation, L.A.S.d.N.; writing—original draft preparation, A.d.N.d.O., L.H.d.O.P., I.M.F., and E.T.L.L.; writing—review and editing, A.d.N.d.O., L.H.d.O.P., F.B.N., D.E.Q.J., L.S.d.S., A.A.F.d.C. and L.A.S.d.N.; visualization, G.N.d.R.F. and L.A.S.d.N.; supervision, C.E.F.d.C., G.N.d.R.F. and L.A.S.d.N.; project administration, L.A.S.d.N.; funding acquisition, G.N.d.R.F. and L.A.S.d.N. All authors have read and agreed to the published version of the manuscript.

**Funding:** This research was funded by Banco da Amazônia grant number 2018/212 and CNPQ, grant number 432221/2018-2.

**Data Availability Statement:** Not applicable.

**Acknowledgments:** The authors would like to thank the laboratories that supported this work: Laboratory of Research and Analysis of Fuels (LAPAC/UFPA), Laboratory of Catalysis and Oil Chemistry (LCO/UFPA) and LABNANO-AMAZON/UFPA. CAPES/UNIFAP, BIORG/UNIFAP and PROPESP/UFPA for the financial support.

**Conflicts of Interest:** The authors declare no conflict of interest.

## References

1. Kresge, C.T.; Roth, W.J. The Discovery of Mesoporous Molecular Sieves from the Twenty Year Perspective. *Chem. Soc. Rev.* **2013**, *42*, 3663–3670. [[CrossRef](#)] [[PubMed](#)]
2. Beck, J.S.; Vartuli, J.C.; Roth, W.J.; Leonowicz, M.E.; Kresge, C.T.; Schmitt, K.D.; Chu, C.T.-W.; Olson, D.H.; Sheppard, E.W.; McCullen, S.B.; et al. A New Family of Mesoporous Molecular Sieves Prepared with Liquid Crystal Templates. *J. Am. Chem. Soc.* **1992**, *27*, 10834–10843. [[CrossRef](#)]
3. Carmo, A.C.; de Souza, L.K.C.; da Costa, C.E.F.; Longo, E.; Zamian, J.R.; da Rocha Filho, G.N. Production of Biodiesel by Esterification of Palmitic Acid over Mesoporous Aluminosilicate Al-MCM-41. *Fuel* **2009**, *88*, 461–468. [[CrossRef](#)]
4. Pires, L.H.O.; Oliveira, A.N.; Monteiro Junior, O.V.; Angélica, R.S.; Costa, C.E.F.; Zamian, J.R.; Nascimento, L.A.S.; Rocha Filho, G.N. Esterification of a Waste Produced from the Palm Oil Industry over 12-Tungstophosphoric Acid Supported on Kaolin Waste and Mesoporous Materials. *Appl. Catal. B Environ.* **2014**, *160–161*, 122–128. [[CrossRef](#)]
5. Sayari, A. Catalysis by Crystalline Mesoporous Molecular Sieves. *Chem. Mater.* **1996**, *8*, 1840–1852. [[CrossRef](#)]
6. Fontes, M.S.B.; Melo, D.M.A.; Costa, C.C.; Braga, R.M.; Melo, M.A.F.; Alves, J.A.B.L.R.; Silva, M.L.P. Effect of Different Silica Sources on Textural Parameters of Molecular Sieve MCM-41. *Cerâmica* **2016**, *62*, 85–90. [[CrossRef](#)]
7. Da Lacerda Júnior, O.S.; Cavalcanti, R.M.; de Matos, T.M.; Venâncio, J.D.B. Synthesis of MCM-41 Mesoporous Material Using Freshwater Sponge as a Source of Silica. *Química Nova* **2013**, *36*, 1348–1353. [[CrossRef](#)]
8. Ciesla, U.; Schüth, F. Ordered Mesoporous Materials. *Microporous Mesoporous Mater.* **1999**, *27*, 131–149. [[CrossRef](#)]
9. Du, C.; Yang, H. Investigation of the Physicochemical Aspects from Natural Kaolin to Al-MCM-41 Mesoporous Materials. *J. Colloid Interface Sci.* **2012**, *369*, 216–222. [[CrossRef](#)]
10. Kumar, P.; Mal, N.; Oumi, Y.; Yamana, K.; Sano, T. Mesoporous Materials Prepared Using Coal Fly Ash as the Silicon and Aluminium Source. *J. Mater. Chem.* **2001**, *11*, 3285–3290. [[CrossRef](#)]
11. Yang, H.; Deng, Y.; Du, C.; Jin, S. Novel Synthesis of Ordered Mesoporous Materials Al-MCM-41 from Bentonite. *Appl. Clay Sci.* **2010**, *47*, 351–355. [[CrossRef](#)]
12. Kang, F.; Wang, Q.; Xiang, S. Synthesis of Mesoporous Al-MCM-41 Materials Using Metakaolin as Aluminum Source. *Mater. Lett.* **2005**, *59*, 1426–1429. [[CrossRef](#)]
13. Madhusoodana, C.D.; Kameshima, Y.; Nakajima, A.; Okada, K.; Kogure, T.; MacKenzie, K.J.D. Synthesis of High Surface Area Al-Containing Mesoporous Silica from Calcined and Acid Leached Kaolinites as the Precursors. *J. Colloid Interface Sci.* **2006**, *297*, 724–731. [[CrossRef](#)]
14. Wang, G.; Wang, Y.; Liu, Y.; Liu, Z.; Guo, Y.; Liu, G.; Yang, Z.; Xu, M.; Wang, L. Synthesis of Highly Regular Mesoporous Al-MCM-41 from Metakaolin. *Appl. Clay Sci.* **2009**, *44*, 185–188. [[CrossRef](#)]
15. De Oliveira, A.N.; Lima, E.T.L.; Oliveira, D.T.; Andrade, E.H.A.; Angélica, R.S.; Costa, C.E.F.; Rocha Filho, G.N.; Costa, F.F.; Luque, R.; Nascimento, L.A.S. Acetylation of Eugenol over 12-Molybdophosphoric Acid Anchored in Mesoporous Silicate Support Synthesized from Flint Kaolin. *Materials* **2019**, *12*, 2995. [[CrossRef](#)]
16. Lima, E.T.L.; Queiroz, L.S.; de Pires, L.H.O.; Angélica, R.S.; Costa, C.E.F.; Zamian, J.R.; Rocha Filho, G.N.; Luque, R.; Nascimento, L.A.S. Valorization of Mining Waste in the Synthesis of Organofunctionalized Aluminosilicates for the Esterification of Waste from Palm Oil Deodorization. *ACS Sustain. Chem. Eng.* **2019**, *7*, 7543–7551. [[CrossRef](#)]
17. De Oliveira, A.N.; Lima, E.T.L.; de Andrade, E.H.A.; Zamian, J.R.; da Rocha Filho, G.N.; da Costa, E.F.; de Pires, L.H.O.; Luque, R.; do Nascimento, L.A.S. Acetylation of Eugenol on Functionalized Mesoporous Aluminosilicates Synthesized from Amazonian Flint Kaolin. *Catalysts* **2020**, *10*, 478. [[CrossRef](#)]

18. De Oliveira, A.N.; de Oliveira, D.T.; Angélica, R.S.; de Andrade, E.H.A.; do Silva, J.K.R.; da Roca Filho, G.N.; Coral, N.; de Pires, L.H.O.; Luque, R.; do Nascimento, L.A.S. Efficient Esterification of Eugenol Using a Microwave-Activated Waste Kaolin. *React. Kinet. Mech. Catal.* **2020**, *130*, 633–653. [[CrossRef](#)]
19. Sun, C.; Zhang, F.; Wang, X.; Cheng, F. Facile Preparation of Ammonium Molybdophosphate/Al-MCM-41 Composite Material from Natural Clay and Its Use in Cesium Ion Adsorption. *Eur. J. Inorg. Chem.* **2015**, *2015*, 2125–2131. [[CrossRef](#)]
20. Sun, C.; Zhang, F.; Li, S.; Cheng, F. Synthesis of SBA-15 Encapsulated Ammonium Molybdophosphate Using Qaidam Natural Clay and Its Use in Cesium Ion Adsorption. *RSC Adv.* **2015**, *5*, 35453–35460. [[CrossRef](#)]
21. Rocha Junior, C.A.F.; Angélica, R.S.; Neves, R.F. Synthesis of Faujasite-type Zeolite: Comparison between Processed and *Flint* Kaolin. *Cerâmica* **2015**, *61*, 259–268. [[CrossRef](#)]
22. Nascimento, L.A.S.; Tito, L.M.Z.; Angélica, R.S.; Costa, C.E.F.; Zamian, J.R.; Rocha Filho, G.N. Esterification of Oleic Acid over Solid Acid Catalysts Prepared from Amazon *Flint* Kaolin. *Appl. Catal. B Environ.* **2011**, *101*, 495–503. [[CrossRef](#)]
23. Carneiro, B.S.; Angélica, R.S.; Scheller, T.; de Castro, E.A.S.; de Neves, R.F. Mineralogical and Geochemical Characterization of the Hard Kaolin from the Capim Region, Pará, Northern Brazil. *Cerâmica* **2003**, *49*, 237–244. [[CrossRef](#)]
24. Nascimento, L.A.S.; Angélica, R.S.; Costa, C.E.F.; Zamian, J.R.; Rocha Filho, G.N. Comparative Study between Catalysts for Esterification Prepared from Kaolins. *Appl. Clay Sci.* **2011**, *51*, 267–273. [[CrossRef](#)]
25. Oliveira, A.N.; da Costa, L.R.S.; Pires, L.H.O.; Nascimento, L.A.S.; Angélica, R.S.; da Costa, C.E.F.; Zamian, J.R.; da Rocha Filho, G.N. Microwave-Assisted Preparation of a New Esterification Catalyst from Wasted *Flint* Kaolin. *Fuel* **2013**, *103*, 626–631. [[CrossRef](#)]
26. Nascimento, L.A.S.; Angélica, R.S.; Costa, C.E.F.; Zamian, J.R.; Rocha Filho, G.N. Conversion of Waste Produced by the Deodorization of Palm Oil as Feedstock for the Production of Biodiesel Using a Catalyst Prepared from Waste Material. *Bioresour. Technol.* **2011**, *102*, 8314–8317. [[CrossRef](#)]
27. Lacerda Júnior, O.S.; Cavalcanti, R.M.; de Matos, T.M.; Angélica, R.S.; da Rocha Filho, G.N.; Barros, I.D.C.L. Esterification of Oleic Acid Using 12-Tungstophosphoric Supported in *Flint* Kaolin of the Amazonia. *Fuel* **2013**, *108*, 604–611. [[CrossRef](#)]
28. Maia, A.A.B.; Saldanha, E.; Angélica, R.S.; Souza, C.A.G.; Neves, R.F. The Use of Kaolin Wastes from the Amazon Region on the Synthesis of Zeolite A. *Cerâmica* **2007**, *53*, 319–324. [[CrossRef](#)]
29. Moraes, C.G.; Rodrigues, E.C.; Neves, R.F. Analcime Zeolite Production from Amazon Kaolin. *Cerâmica* **2013**, *59*, 563–569. [[CrossRef](#)]
30. Khayoon, M.S.; Hameed, B.H. Single-Step Esterification of Crude Karanj (*Pongamia Pinnata*) Oil to Fatty Acid Methyl Esters over Mesoporous SBA-16 Supported 12-Molybdophosphoric Acid Catalyst. *Fuel Process. Technol.* **2013**, *114*, 12–20. [[CrossRef](#)]
31. Oliveira, A.N.; Lima, M.A.B.; Pires, L.H.O.; Silva, M.R.; Luz, P.T.S.; Angélica, R.S.; Rocha Filho, G.N.; Costa, C.E.F.; Luque, R.; Nascimento, L.A.S. Bentonites Modified with Phosphomolybdic Heteropolyacid (HPMo) for Biowaste to Biofuel Production. *Materials* **2019**, *12*, 1431. [[CrossRef](#)] [[PubMed](#)]
32. Wang, H.; Liu, L.; Gong, S. Esterification of Oleic Acid to Biodiesel over a 12-Phosphotungstic Acid-Based Solid Catalyst. *J. Fuel Chem. Technol.* **2017**, *45*, 303–310. [[CrossRef](#)]
33. Carvalho, A.K.F.; Conceição, L.R.V.; Silva, J.P.V.; Perez, V.H.; de Castro, H.F. Biodiesel Production from *Mucor Circinelloides* Using Ethanol and Heteropolyacid in One and Two-step Transesterification. *Fuel* **2017**, *202*, 503–511. [[CrossRef](#)]
34. Conceição, L.R.V.; Carneiro, L.M.; Giordani, D.S.; de Castro, H.F. Synthesis of Biodiesel from Macaw Palm Oil Using Mesoporous Solid Catalyst Comprising 12-Molybdophosphoric Acid and Niobia. *Renew. Energy* **2017**, *113*, 119–128. [[CrossRef](#)]
35. Brahmkhatri, V.; Patel, A. An Efficient Green Catalyst Comprising 12-Tungstophosphoric Acid and MCM-41: Synthesis Characterization and Diesterification of Succinic Acid, a Potential Bio-platform Molecule. *Green Chem. Lett. Rev.* **2012**, *5*, 161–171. [[CrossRef](#)]
36. Clemente, M.C.H.; Martins, G.A.V.; de Freitas, E.F.; Dias, J.A.; Dias, S.C.L. Ethylene Production via Catalytic Ethanol Dehydration by 12-Tungstophosphoric Acid@ceria-Zirconia. *Fuel* **2019**, *239*, 491–501. [[CrossRef](#)]
37. Patel, A.; Brahmkhatri, V. Kinetic Study of Oleic Acid Esterification over 12-Tungstophosphoric Acid Catalyst Anchored to Different Mesoporous Silica Supports. *Fuel Process. Technol.* **2013**, *113*, 141–149. [[CrossRef](#)]
38. Brahmkhatri, V.; Patel, A. 12-Tungstophosphoric Acid Anchored to SBA-15: An Efficient, Environmentally Benign Reusable Catalysts for Biodiesel Production by Esterification of Free Fatty Acids. *Appl. Catal. A Gen.* **2011**, *403*, 161–172. [[CrossRef](#)]
39. Mongkolbovornkij, P.; Champreda, V.; Sutthisripok, W.; Laosiripojana, N. Esterification of Industrial-Grade Palm Fatty Acid Distillate over Modified ZrO<sub>2</sub> (with WO<sub>3</sub>-, SO<sub>4</sub>- and TiO<sub>2</sub>-): Effects of Co-solvent Adding and Water Removal. *Fuel Process. Technol.* **2010**, *91*, 1510–1516. [[CrossRef](#)]
40. Da Conceição, R.L.V.; Carneiro, L.M.; Rivaldi, J.D.; de Castro, H.F. Solid Acid as Catalyst for Biodiesel Production via Simultaneous Esterification and Transesterification of Macaw Palm Oil. *Ind. Crop. Prod.* **2016**, *89*, 416–424. [[CrossRef](#)]
41. Akinfalabi, S.I.; Rashid, U.; Yunus, R.; Taufiq-Yap, Y.H. Synthesis of Biodiesel from Palm Fatty Acid Distillate Using Sulfonated Palm Seed Cake Catalyst. *Renew. Energy* **2017**, *111*, 611–619. [[CrossRef](#)]
42. Lokman, I.M.; Rashid, U.; Taufiq-Yap, Y.H. Production of Biodiesel from Palm Fatty Acid Distillate Using Sulfonated-Glucose Solid Acid Catalyst: Characterization and Optimization. *Chin. J. Chem. Eng.* **2015**, *23*, 1857–1864. [[CrossRef](#)]
43. Soltani, S.; Rashid, U.; Yunus, R.; Taufiq-Yap, Y.H. Biodiesel Production in the Presence of Sulfonated Mesoporous ZnAl<sub>2</sub>O<sub>4</sub> Catalyst via Esterification of Palm Fatty Acid Distillate (PFAD). *Fuel* **2016**, *178*, 253–262. [[CrossRef](#)]

44. Embong, N.H.; Maniam, G.P.; Mohd, M.H.; Lee, K.T.; Huisingh, D. Utilization of Palm Fatty Acid Distillate in Methyl Esters Preparation Using  $\text{SO}_4^{2-}/\text{TiO}_2\text{-SiO}_2$  as a Solid Acid Catalyst. *J. Clean. Prod.* **2016**, *116*, 244–248. [[CrossRef](#)]
45. Pantoja, S.S.; de Mescouto, V.A.; da Costa, C.E.F.; Zamian, J.R.; Zamian, J.R.; da Rocha Filho, G.N.; do Nascimento, L.A.S. High-Quality Biodiesel Production from Buriti (*Mauritia Flexuosa*) Oil Soapstock. *Molecules* **2019**, *24*, 94. [[CrossRef](#)]
46. Lima, R.P.; da Luz, P.T.S.; Braga, M.; dos Batista, P.R.S.; da Costa, C.E.F.; Zamian, J.R.; do Nascimento, L.A.S.; da Rocha Filho, G.N. Murumuru (*Astrocaryum Murumuru* Mart.) Butter and Oils of Buriti (*Mauritia Flexuosa* Mart.) and Pracaxi (*Pentaclethra Macroloba* (Willd.) Kuntze) can be Used for Biodiesel Production: Physico-Chemical Properties and Thermal and Kinetic Studies. *Ind. Crop. Prod.* **2017**, *97*, 536–544. [[CrossRef](#)]
47. Aboim, J.B.; de Oliveira, D.T.; Ferreira, J.E.; Siqueira, A.S.; Dall’Agnol, L.T.; da Rocha, G.N.; Gonçalves, E.C.; Nascimento, L.A.S. Determination of Biodiesel Properties Based on a Fatty Acid Profile of Eight Amazon Cyanobacterial Strains Grown in Two Different Culture Media. *RSC Adv.* **2016**, *6*, 109751–109758. [[CrossRef](#)]
48. De Oliveira, D.T.; Vasconcelos, C.; Feitosa, A.M.T.; Aboim, J.B.; de Oliveira, A.N.; Xavier, L.P.; Santos, A.S.; Gonçalves, E.C.; da Rocha Filho, G.N.; do Nascimento, L.A.S. Lipid Profile Analysis of Three New Amazonian Cyanobacteria as Potential Sources of Biodiesel. *Fuel* **2018**, *234*, 785–788. [[CrossRef](#)]
49. Aguiéiras, E.C.G.; Souza, S.L.; Langone, M.A.P. Study of Immobilized Lipase Lipozyme RM IM in Esterification Reactions for Biodiesel Synthesis. *Quím. Nova* **2013**, *36*, 646–650. [[CrossRef](#)]
50. Bastos, R.R.C.; da Luz Corrêa, A.P.; da Luz, P.T.S.; da Rocha Filho, G.N.; Zamian, J.R.; da Conceição, L.R.V. Optimization of Biodiesel Production Using Sulfonated Carbon-Based Catalyst from an Amazon Agro-Industrial Waste. *Energy Convers. Manag.* **2020**, *205*, 112457. [[CrossRef](#)]
51. Da Corrêa, A.P.L.; Bastos, R.R.C.; da Rocha Filho, G.N.; Zamian, J.R.; da Conceição, L.R.V. Preparation of Sulfonated Carbon-Based Catalysts from Murumuru Kernel Shell and Their Performance in the Esterification Reaction. *RSC Adv.* **2020**, *10*, 20245–20256. [[CrossRef](#)]
52. Wan, Z.; Lim, J.K.; Hameed, B.H. Chromium-Tungsten Heterogeneous Catalyst for Esterification of Palm Fatty Acid Distillate to Fatty Acid Methyl Ester. *J. Taiwan Inst. Chem. Eng.* **2015**, *54*, 64–70. [[CrossRef](#)]
53. Da Conceição, L.R.V.; Reis, C.E.R.; de Lima, R.; Cortez, D.V.; de Castro, H.F. Keggin-Structure Heteropolyacid Supported on Alumina to be Used in Trans/Esterification of High-Acid Feedstocks. *RSC Adv.* **2019**, *9*, 23450–23458. [[CrossRef](#)]
54. Aranda, D.A.G.; Santos, R.T.P.; Tapanes, N.C.O.; Ramos, A.L.D.; Antunes, O.A.C. Acid-Catalyzed Homogeneous Esterification Reaction for Biodiesel Production from Palm Fatty Acids. *Catal. Lett.* **2008**, *122*, 20–25. [[CrossRef](#)]
55. Peruzzolo, T.M.; Stival, J.F.; Baika, L.M.; Ramos, L.P.; Grassi, M.T.; Rocco, M.L.M.; Nakagaki, S. Efficient Esterification Reaction of Palmitic Acid Catalyzed by  $\text{WO}_3-x$ /Mesoporous Silica. *Biofuels* **2020**, 1–11. [[CrossRef](#)]
56. Wan, Z.; Hameed, B.H. Chromium-Tungsten-Titanium Mixed Oxides Solid Catalyst for Fatty Acid Methyl Ester Synthesis from Palm Fatty Acid Distillate. *Energy Convers. Manag.* **2014**, *88*, 669–676. [[CrossRef](#)]
57. Araujo, R.O.; da Char, J.S.; Queiroz, L.S.; da Rocha Filho, G.N.; da Costa, C.E.F.; da Silva, G.C.T.; Landers, R.; Costa, M.J.F.; Gonçalves, A.A.S.; de Souza, L.K.C. Low Temperature Sulfonation of Acai Stone Biomass Derived Carbons as Acid Catalysts for Esterification Reactions. *Energy Convers. Manag.* **2019**, *196*, 821–830. [[CrossRef](#)]
58. Olutoye, M.A.; Wong, C.P.; Chin, L.H.; Hameed, B.H. Synthesis of FAME from the Methanolysis of Palm Fatty Acid Distillate Using Highly Active Solid Oxide Acid Catalyst. *Fuel Process. Technol.* **2014**, *124*, 54–60. [[CrossRef](#)]
59. Chabukswar, D.D.; Heer, P.K.K.S.; Gaikar, V.G. Esterification of Palm Fatty Acid Distillate Using Heterogeneous Sulfonated Microcrystalline Cellulose Catalyst and Its Comparison with  $\text{H}_2\text{SO}_4$  Catalyzed Reaction. *Eng. Chem. Res.* **2013**, *52*, 7316–7326. [[CrossRef](#)]
60. Wimonrat, T. Supported Cesium Polyoxotungstates as Catalysts for the Esterification of Palm Fatty Acid Distillate. *Mendeleev Commun.* **2013**, *23*, 46–48. [[CrossRef](#)]
61. Oliveira, C.F.; Dezaneti, L.M.; Garcia, F.A.C.; de Macedo, J.L.; Dias, J.A.; Dias, S.C.L.; Alvim, K.S.P. Esterification of Oleic Acid with Ethanol by 12-Tungstophosphoric Acid Supported on Zirconia. *Appl. Catal. A Gen.* **2010**, *372*, 153–161. [[CrossRef](#)]
62. Méndez, F.J.; Llanos, A.; Echeverría, M.; Jáuregui, R.; Villasana, Y.; Díaz, Y.; Liendo-Polanco, G.; Ramos-García, M.A.; Zoltan, T.; Brito, J.L. Mesoporous Catalysts Based on Keggin-Type Heteropolyacids Supported on MCM-41 and Their Application in Thiophene Hydrodesulfurization. *Fuel* **2013**, *110*, 249–258. [[CrossRef](#)]
63. Morey, M.S.; Bryan, J.D.; Schwarz, S.; Stucky, G.D. Pore Surface Functionalization of MCM-48 Mesoporous Silica with Tungsten and Molybdenum Metal Centers: Perspectives on Catalytic Peroxide Activation. *Chem. Mater.* **2000**, *12*, 3435–3444. [[CrossRef](#)]
64. Pacula, A.; Pamin, K.; Krysiak-Czerwenka, J.; Olejniczak, Z.; Gil, B.; Bielanska, E.; Dula, R.; Serwicka, E.M.; Drelinkiewicz, A. Physicochemical and Catalytic Properties of Hybrid Catalysts Derived from 12-Molybdophosphoric Acid and Montmorillonites. *Appl. Catal. A Gen.* **2015**, *498*, 192–204. [[CrossRef](#)]
65. Vazquez, P.G.; Blanco, M.N.; Caceres, C.V. Catalysts Based on Supported 12-Molybdophosphoric Acid. *Catal. Lett.* **1999**, *60*, 205–215. [[CrossRef](#)]
66. Melero, J.A.; Bautista, L.F.; Morales, G.; Iglesias, J.; Sánchez-Vázquez, R. Biodiesel Production from Crude Palm Oil Using Sulfonic Acid-Modified Mesostructured Catalysts. *Chem. Eng. J.* **2010**, *161*, 323–331. [[CrossRef](#)]
67. Melero, J.A.; Bautista, L.F.; Iglesias, J.; Morales, G.; Sánchez-Vázquez, R.; Wilson, K.; Lee, A.F. New Insights in the Deactivation of Sulfonic Modified SBA-15 Catalysts for Biodiesel Production from Low-Grade Oleaginous Feedstock. *Appl. Catal. A Gen.* **2014**, *488*, 111–118. [[CrossRef](#)]